Title

Gamma secretase activity modulates BMP-7-induced dendritic growth in primary rat sympathetic neurons

Authors

Karunungan, Krystal
Garza, Rachel H
Grodzki, Ana Cristina
et al.

Publication Date

2023-07-01

DOI

10.1016/j.autneu.2023.103085

Autonomic Neuroscience: Basic and Clinical 247 (2023) 103085

Contents lists available at ScienceDirect

Autonomic Neuroscience: Basic and Clinical

journal homepage: www.elsevier.com/locate/autneu

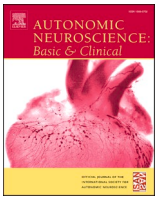

Gamma secretase activity modulates BMP-7-induced dendritic growth in primary rat sympathetic neurons

Krystal Karunungan [a], Rachel H. Garza [a], Ana Cristina Grodzki [b], Megan Holt [a], Pamela J. Lein [b], Vidya Chandrasekaran [a,*]

[a] Department of Biology, Saint Mary's College of California, 1928 Saint Mary's Road, Moraga, CA 94556, United States of America
[b] Department of Molecular Biosciences, University of California, Davis, 1089 Veterinary Medicine Drive, Davis, CA 95616, United States of America

ARTICLE INFO

Keywords:
γ-Secretase
DAPT
LY-411575
BMS-299897
Dendrite
Bone morphogenetic proteins
Sympathetic neurons
Presenilin

ABSTRACT

Autonomic dysfunction has been observed in Alzheimer's disease (AD); however, the effects of genes involved in AD on the peripheral nervous system are not well understood. Previous studies have shown that presenilin-1 (PSEN1), the catalytic subunit of the gamma secretase (γ-secretase) complex, mutations in which are associated with familial AD function, regulates dendritic growth in hippocampal neurons. In this study, we examined whether the γ-secretase pathway also influences dendritic growth in primary sympathetic neurons. Using immunoblotting and immunocytochemistry, molecules of the γ-secretase complex, PSEN1, PSEN2, PEN2, nicastrin and APH1a, were detected in sympathetic neurons dissociated from embryonic (E20/21) rat sympathetic ganglia. Addition of bone morphogenetic protein-7 (BMP-7), which induces dendrites in these neurons, did not alter expression or localization of γ-secretase complex proteins. BMP-7-induced dendritic growth was inhibited by siRNA knockdown of PSEN1 and by three γ-secretase inhibitors, γ-secretase inhibitor IX (DAPT), LY-411575 and BMS-299897. These effects were specific to dendrites and concentration-dependent and did not alter early downstream pathways of BMP signaling. In summary, our results indicate that γ-secretase activity enhances BMP-7 induced dendritic growth in sympathetic neurons. These findings provide insight into the normal cellular role of the γ-secretase complex in sympathetic neurons.

1. Introduction

Alzheimer's disease is characterized by the accumulation of neurofibrillary tangles and plaques in the brain (Hane et al., 2017; Tanzi et al., 2001). Two major mutations associated with familial Alzheimer's disease are dominant loss of function mutations in presenilin 1 (PSEN1) and presenilin 2 (PSEN2), both of which are proteins in the γ-secretase complex (Haass and de Strooper, 1999; Tanzi et al., 2001; Zoltowska and Berezovska, 2017). γ-Secretase is a large complex consisting of four core proteins: presenilin (PSEN1 or PSEN2), which is the catalytic subunit, nicastrin (NCT), anterior pharynx defective-1 (APH-1) and presenilin enhancer-2 (PEN2) (Carroll and Li, 2016; Francis et al., 2002; Gu et al., 2004; Li et al., 2014; Zhang et al., 2014). This complex is involved in proteolysis of over 90 proteins within the transmembrane domain, including amyloid precursor protein (APP), Notch, Ephrins, Cadherins and $p75^{NTR}$ (Carroll and Li, 2016; Haapasalo and Kovacs, 2011; Wolfe, 2002; Zhang et al., 2014). Many of the substrates of γ-secretase have been implicated in various aspects of neuronal development including neurite outgrowth, synaptogenesis, dendritic growth and neuronal survival (Haapasalo and Kovacs, 2011).

Three lines of evidence suggest a potential role of the γ-secretase complex in dendritogenesis in the central nervous system: (1) PSEN1 is known to be localized to the somatodendritic compartment in human neuronal cell lines and rat central neurons, suggesting that it might have a role in dendritogenesis (Busciglio et al., 1997; Cook et al., 1996); (2) PSEN knockout mice show loss of dendritic arbor and spine density in cortical and hippocampal neurons (Lee and Aoki, 2012; Saura et al., 2004); and (3) a recent study showed that γ-secretase inhibition resulted in an APP-dependent increase in axo-dendritic sprouting in cortical neurons (Deyts et al., 2016).

Emerging data suggest that autonomic dysfunction, especially impairment of the sympathetic nervous system, is observed during early

Abbreviations: BMP, bone morphogenetic proteins; TGF-β, transforming growth factor-beta; SCG, superior cervical ganglia; NGF, nerve growth factor; GAPDH, glyceraldehyde phosphate dehydrogenase; γ-secretase, gamma secretase.

* Corresponding author at: Department of Biology, Saint Mary's College of California, Moraga, CA 94556, United States of America.
E-mail address: vc5@stmarys-ca.edu (V. Chandrasekaran).

https://doi.org/10.1016/j.autneu.2023.103085
Received 16 December 2022; Received in revised form 28 March 2023; Accepted 29 March 2023
Available online 6 April 2023

stages of Alzheimer's disease and may contribute to disease pathology (Engelhardt and Laks, 2008; Femminella et al., 2014; Issac et al., 2017; Jensen-Dahm et al., 2015). Currently, there is limited knowledge of the role of the γ-secretase complex in the sympathetic nervous system. One study has shown that activation of $p75^{NTR}$ following γ-secretase cleavage in PC12 cells and postnatal superior cervical ganglia neurons regulates cell survival downstream of nerve growth factor signaling (Bengoechea et al., 2009). Another study demonstrated that treatment with a γ-secretase inhibitor increased the accumulation of gangliosides at neuritic terminals, suggesting that this complex may be important for neuronal membrane structure (Oikawa et al., 2012). Understanding the normal cellular roles of genes involved in Alzheimer's disease pathogenesis in the peripheral nervous system would provide further insight into the biology of Alzheimer's disease. The goal of this study is to explore the contribution of the γ-secretase pathway to dendritogenesis in the sympathetic nervous system.

Previous studies have shown that members of the bone morphogenetic protein (BMP) family are positive regulators of dendritic growth in central and peripheral neurons (Angley et al., 2003; Esquenazi et al., 2002; Granholm et al., 1999; Gratacos et al., 2008; Guo et al., 1998; Hocking et al., 2008; le Roux et al., 1999; Lein et al., 1995; Majdazari et al., 2013; Withers et al., 2000). BMPs have been shown to mediate their effects on dendritic growth through binding to their cognate receptors (BMPRs), which then leads to the activation and nuclear translocation of SMAD proteins to activate transcription (Angley et al., 2003; Garred et al., 2011; Guo et al., 1998; Massagué and Chen, 2000). Studies have shown that interactions between BMP signaling and other signaling pathways such as cytokine signaling, retinoic acid signaling and free radical mediated pathways help shape the dendritic arbor in peripheral neurons (reviewed in Chandrasekaran and Lein, 2018). Interestingly, increased expression of BMP-6 and BMP-4 have been observed in the brains of Alzheimer's disease patients, and in mouse models of Alzheimer's disease (Crews et al., 2010; Li et al., 2008). However, the potential interactions between γ-secretase and the BMP signaling pathway to regulate dendritogenesis in sympathetic neurons are not understood.

Therefore, in this study, we test the hypothesis that γ-secretase activity modulates BMP-induced dendritic growth in sympathetic neurons. Our data show that members of the γ-secretase complex are expressed in peripheral neurons and inhibition of γ-secretase activity significantly decreases BMP-7-induced dendritic growth in sympathetic neurons *in vitro*.

2. Materials and methods

2.1. Materials

Recombinant human bone morphogenetic proteins (BMPs) were generously provided by Curis (Cambridge, MA, USA). γ-Secretase inhibitors LY-411575, γ-secretase inhibitor IX (DAPT) and BMS-2998987 were purchased from Millipore-Sigma, (St. Louis, MO). PSEN1 siRNA (sc-36312, Santa Cruz Biotechnology (Dallas, TX) contains a mixture of three 19–25 bp sequences that bind the target mRNA). Scrambled control siRNA (sc-37007) was also obtained from Santa Cruz Biotechnology. Other tissue culture media components and gel electrophoresis supplies were purchased from Life Technologies (Grand Island, NY).

2.2. Animals

All procedures involving animals were done in accordance with the Institutional Review Board of the University of California, Davis (Davis, CA) or Saint Mary's College of California (Moraga, CA) and were in compliance with the NIH guidelines for animal care and use. Timed-pregnant Sprague Dawley rats purchased from Charles River Laboratories (Hollister, CA) were housed in temperature controlled (22 ± 2 °C) plastic cages on a 12 h light-dark cycle. Food and water were provided *ad libitum*. Pregnant rats were humanely euthanized using carbon dioxide prior to removal of the E21 pups from the uterine and amniotic sacs for dissection of the superior cervical ganglia; no experimental manipulation occurred prior to euthanasia. P0 pups were euthanized using carbon dioxide, prior to the removal of the superior cervical ganglia.

2.3. Culturing sympathetic neurons

Sympathetic neurons were dissociated from the SCG of embryonic (E20/21/P0) Sprague-Dawley rat pups according to previously described protocols (Ghogha et al., 2012; Holt et al., 2020). Cells were plated onto 24-well plates with or without glass coverslips (Ted Pella, Redding, CA) pretreated with 100 μg/mL of poly-D-lysine (BD Biosciences, San Jose, CA). Cultures were maintained in serum-free media (50:50 v/v DMEM:F12, Thermo Fisher Scientific, Waltham, MA) containing β-nerve growth factor (NGF, 100 ng/mL, Harlan Laboratories, Indianapolis, IN), bovine serum albumin (BSA, 500 μg/mL, Millipore-Sigma, Burlington, MA), bovine insulin (10 μg/mL, Thermo Fisher Scientific, Waltham, MA) and human transferrin (10 μg/mL, Thermo Fisher Scientific, Waltham, MA) at 35 °C in a humidified chamber containing 5 % CO_2. To eliminate non-neuronal cells, cultures were treated with cytosine-β-D-arabinofuranoside (Ara-C, 2 μM, Millipore-Sigma, St. Louis, MO) for 48 h beginning 1 d after plating. The neuronal cell cultures were then subjected to experimental treatments as described below.

2.4. Transfection of sympathetic neurons with PSEN1 siRNA

Following the elimination of non-neuronal cells, cultured embryonic sympathetic neurons were transfected with 60 pmol of Scrambled control siRNA or 60 pmol of PSEN1 siRNA using Lipofectamine® RNAiMAX siRNA Transfection Reagent (Thermo Fisher Scientific, Waltham, MA) per the manufacturer's instructions modified such that cultures were incubated with the transfection mixture for only 6–7 h. As an additional control, a subset of cultures was similarly exposed to transfection reagent without the addition of any siRNA. After the incubation period, cells were rinsed and maintained in serum-free medium (described above) overnight. The following day, the transfected neurons were treated with growth medium in the absence or presence of BMP-7 (50 ng/mL) for 5 d to induce dendritic growth. The cultures were then fixed and immunostained for morphological analyses as described below. The knockdown of PSEN1 protein following transfection was examined by immunocytochemistry using three different PSEN1 antibodies [PSEN1 antibody (EP2000Y 1:500, Abcam), D39D1 (1:1000, Cell Signaling Technology) and D10 (1:250, Thermo Fisher Scientific)] visualized by indirect immunofluorescence. Immunostained neurons were imaged using a Leica Stellaris confocal microscope. The laser settings (intensity and gain) were maintained at constant values between the different conditions to allow comparison between the levels of PSEN1 protein in neurons treated with control siRNA *vs.* PSEN1 siRNA.

2.5. Morphological analyses

To quantify dendritic growth, neurons were fixed with 4 % paraformaldehyde, immunostained using an antibody against microtubule associated protein 2 (SMI-52, MAP-2; 1:5000, Millipore, Billerica, MA), which specifically labels the cell body and dendrites, and visualized using immunofluorescence (Ghogha et al., 2012). The fluorescent images were acquired using the Nikon Eclipse E400 fluorescence microscope and SPOT camera. Dendritic morphology was quantified in digitized images of neurons immunopositive for MAP-2 using Image J (version 1.48, NIH).

To quantify axonal growth, neurons were fixed with 4 % paraformaldehyde, immunostained using an antibody against the phosphorylated forms of M and H neurofilaments (SMI-31, 1:1000, BioLegend, San Diego CA) which labels cell bodies and axons and visualized using immunofluorescence. Images were acquired using the

ImageXpress Micro XL high-content imaging system (Molecular Devices, Sunnyvale, CA, USA) with 10× magnification, and automated image analysis was performed using MetaXpress software (Molecular Devices, versions 5.3 and 6.2, RRID:SCR_016654). Quality control was run on all images; those that were not in focus were discarded. BMP-7 or C2 controls were run with each data set to determine thresholds for analysis. 4 to 19 images were randomly taken at 10× from each of the 3–4 coverslips per treatment.

2.6. Immunocytochemical localization of γ-secretase complex and SMADs

To localize the γ-secretase complex in sympathetic neurons, neuronal cell cultures were treated in the presence or absence of BMP-7 (50 ng/mL) for 5 d, fixed with 4 % paraformaldehyde and immunostained for presenilin 1 (PSEN1), presenilin 2 (PSEN2), nicastrin, PEN2 or APH1a, and visualized using indirect immunofluorescence. The following primary antibodies were used: rabbit anti-PSEN1 (EP2000Y, 1:500, Abcam, Cambridge, MA), rabbit anti-PSEN2 (ab51249, 1:100, Abcam, Cambridge, MA), rabbit anti-nicastrin (ab45425, 1:50, Abcam, Cambridge, MA), mouse anti-PEN2 (1C12-G5, 1:10, Santa Cruz Biotechnology, Dallas, TX) and rabbit anti-APH1a (ab12104, 1:50, Abcam, Cambridge, MA). The cultures were co-stained with mouse anti-MAP-2 antibody (SMI-52, 1:5000) to visualize dendrites. Alexa dye conjugated goat anti-rabbit (1:1000, Thermo Fisher Scientific, Waltham, MA) and goat-anti-mouse (1:1000, Thermo Fisher Scientific, Waltham, MA) were used as the secondary antibodies. The antibodies have been previously used to detect members of the γ-secretase complex (D'Souza et al., 2015; Wang et al., 2015; Zhang et al., 2018). The immunofluorescence was imaged using the Leica Stellaris 5 confocal microscope (Leica Microsystems, Deerfield, IL).

To detect phospho-SMAD 1,5, neurons were treated on day *in vitro* (DIV) 4–5 with BMP-7 (50 ng/mL) in the presence or absence of the γ-secretase inhibitors for 5 d. Subcellular distribution of SMAD1 was assessed in cultures immunostained for phosphorylated SMAD 1,5 (41D10, 1:100 dilution, Cell Signaling Technology) and visualized using indirect immunofluorescence as previously described (Kim et al., 2009).

2.7. Western blotting

SCG cultures treated in the presence or absence of 50 ng/mL BMP-7 for 5 d were lysed in buffer containing 20 mM HEPES (pH 7.4), 150 mM sodium chloride, 1 % Triton X-100, 10 % glycerol, 2 mM EGTA and 1× Protease Inhibitor cocktail (Millipore, Billerica, MA). Lysates were heated to 70 °C in 4× LDS sample buffer (Life Technologies, Grand Island, NY) and centrifuged. Protein concentrations were determined using Bradford Protein Assay and an equal amount of protein from each condition was subjected to gel electrophoresis for 1.5 h at 200 V, in accordance with the manufacturer's protocol (Thermo Fisher Scientific, Waltham, MA). The proteins were transferred to a nitrocellulose membrane (Thermo Fisher Scientific, Waltham, MA) at 11 V overnight in 4 °C. The membrane was blocked in 5 % dried nonfat milk powder (Safeway) with 0.1 % TWEEN 20 in PBS for 1 h at room temperature on a shaker. The following primary antibodies were used: rabbit anti-PSEN1 (EP2000Y, 1:500, Abcam, Cambridge, MA), rabbit anti-PSEN2 (1:100, Abcam), rabbit anti-nicastrin (1:50, Abcam), mouse anti-PEN2 (1:10) and rabbit anti-APH1a (1:50, Abcam), rabbit anti-PSEN1 CTF (D39D1,

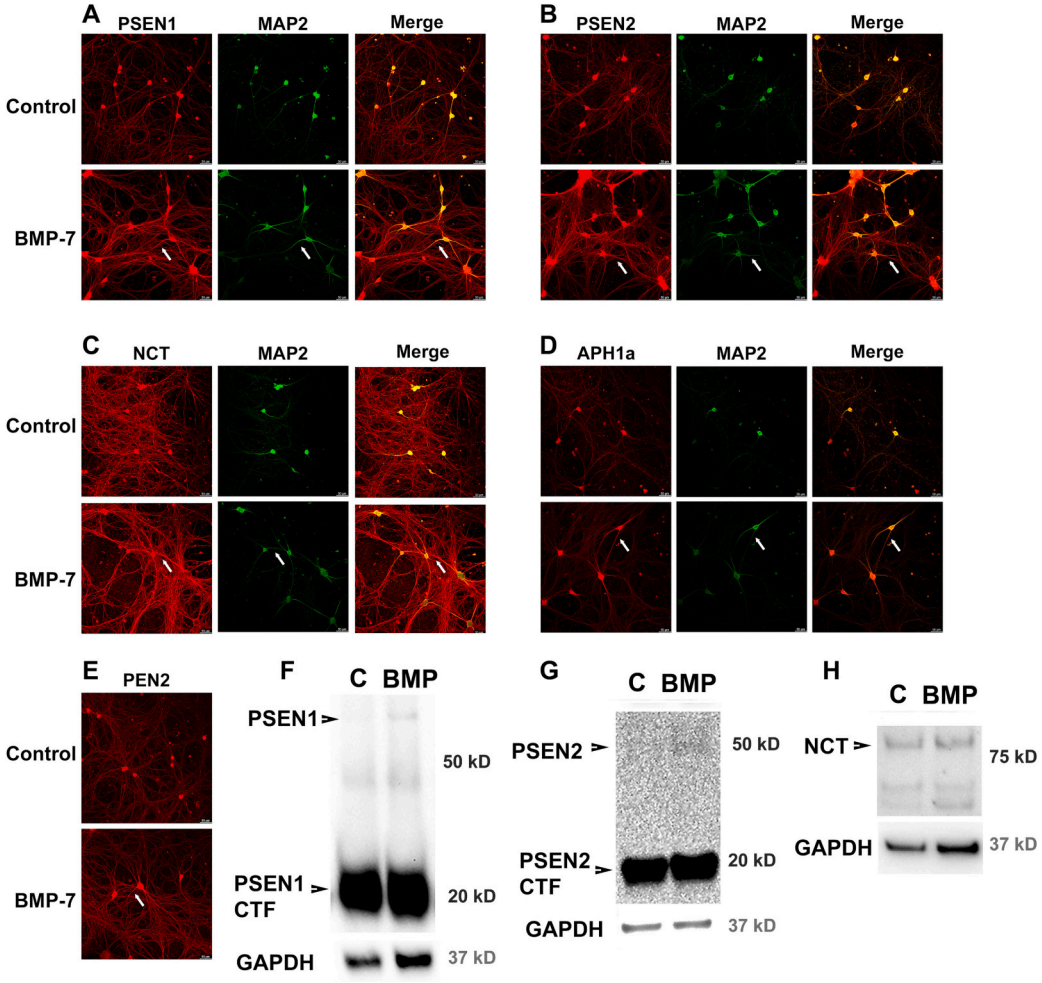

Fig. 1. The components of the γ-secretase complex are expressed in primary rat sympathetic neurons. Sympathetic neurons cultured from E21 rat pups were grown in the absence (labeled — Control) or presence of BMP-7 (50 ng/ml) (labeled BMP-7) for 5 d, following elimination of non-neuronal cells. Panels A–E show representative images of the immunocytochemical localization of five components of the γ-secretase complex, PSEN1 (A), PSEN2 (B), NCT (C), APH1a (D), PEN2 (E) in red, staining for microtubule associated-protein-2 (MAP2) to show the dendrites in green (A–D) and the merge of the two channels (A–D) to show colocalization of the γ-secretase complex with dendrites. Immunoblotting was performed to confirm the expression of PSEN1 (F), PSEN2 (G) and NCT (H). C = control. The white arrow in each panel points to a dendrite. (For interpretation of the references to color in this figure legend, the reader is referred to the web version of this article.)

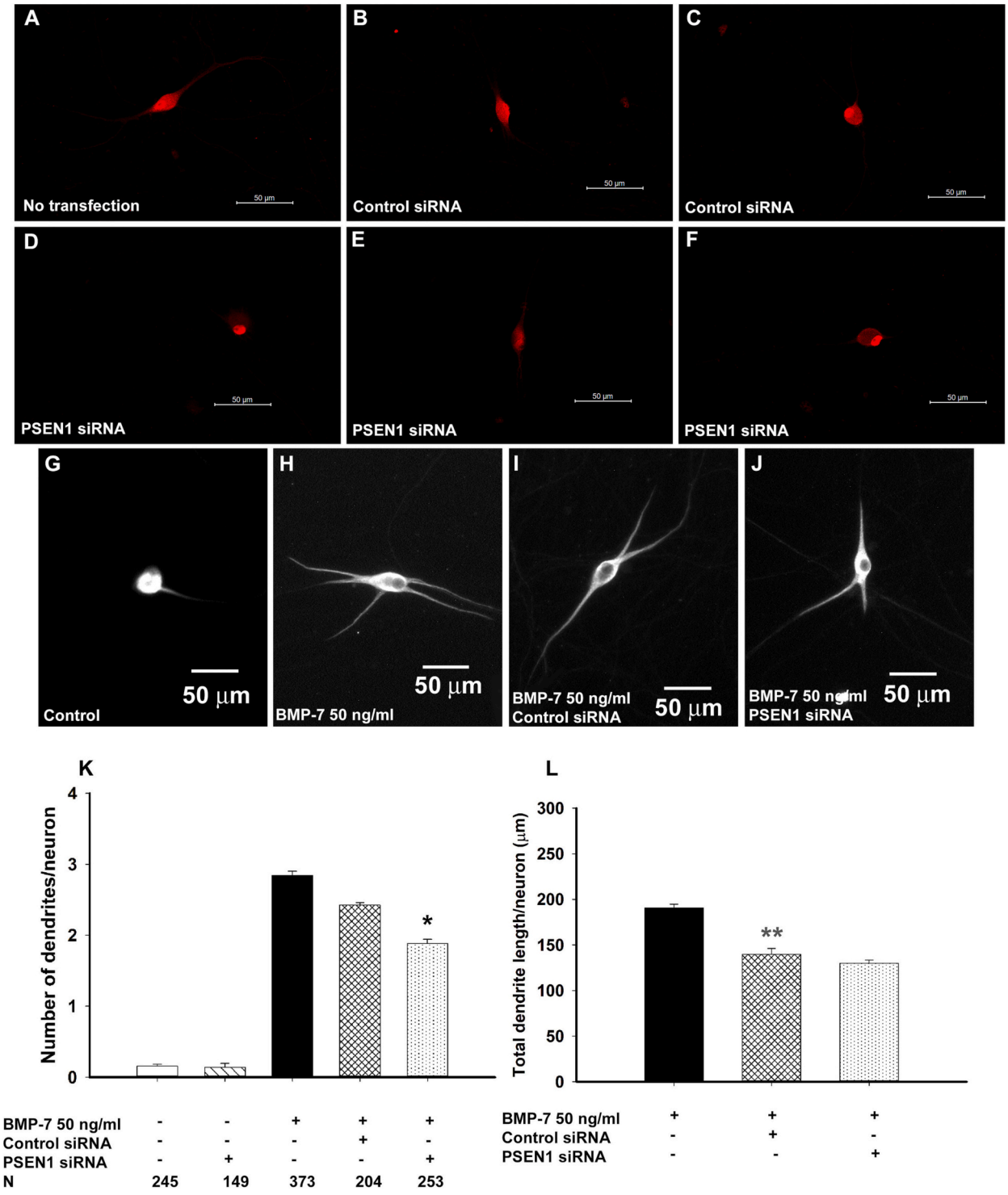

Fig. 2. PSEN1 siRNA decreases dendritic growth in primary sympathetic neurons. Representative photomicrographs showing PSEN1 immunoreactivity in sympathetic neurons treated with BMP-7 (50 ng/mL) without transfection (A), transfected with control siRNA (B, C) or transfected with PSEN1 siRNA (D–F). The images were taken at constant exposure. Representative photomicrographs of MAP-2 immunoreactivity in primary sympathetic neurons subjected to the transfection protocol in the absence of any siRNA (H) or in the presence of control (scrambled) siRNA (I) or PSEN1 siRNA (J) prior to BMP-7 treatment for 5 d. Control cultures (G) were maintained in the absence of BMP-7. Dendritic growth was quantified with respect to the number of primary dendrites per neuron (K) and the total dendritic length per neuron (L). Data are presented as the mean ± SEM. The number of cells analyzed (N) is listed in the figure. Statistical significance was determined by one-way ANOVA followed by Tukey's *post hoc* comparison test. *Significantly different at $p \leq 0.05$ compared to neurons treated with BMP-7 with control siRNA transfection. **Significantly different at $p \leq 0.05$ compared to neurons treated with BMP-7 (no transfection).

1:1000, Cell Signaling Technology), with HRP-conjugated goat anti-rabbit IgG (1:1000, Chemicon, Waltham, MA) as the secondary antibody. GAPDH was used as a loading control and its protein levels were assessed using a rabbit anti-GAPDH (14C10, 1:1000), Cell Signaling Technology). The blots were then visualized using enhanced chemiluminescence (Sigma, St. Louis, MO) and imaged using ChemiDoc XRS® (Bio-Rad Laboratories, Hercules, CA).

Axonal growth was assessed using western blotting with a mouse monoclonal antibody against the phosphorylated forms of M and H neurofilaments (SMI-31, 1:1000, Millipore, Billerica, MA), which are selectively localized to axons (Lein et al., 2007). On DIV 4–5, SCG cultures were treated for 5 d with control medium or medium supplemented with BMP-7 (50 ng/mL) in the absence or presence of one of the two γ-secretase inhibitors, DAPT (10 μM) or LY-411575 (10 μM). The cultures were lysed and subjected to western blot analyses as described above.

2.8. Measurement of cell viability

After non-neuronal cells were eliminated, neuronal cell cultures were treated for 5 d with control medium or medium supplemented with BMP-7 (50 ng/mL) in the absence or presence of DAPT (30 μM), LY-411575 (10 μM) or vehicle control (DMSO diluted 1:1000). Viability was assessed by using the MTT assay to measure reducing capability. Cultures were incubated with 3-(4,5-dimethyl-2-thiazolyl)-2,5-diphenyl-2H-tetrazolium bromide (MTT) at 500 μg/mL for 4 h at 37 °C. The purple formazan was dissolved in 200 μL of DMSO and absorbance was measured at 560 nm on a Tecan Infinite® F200 Spectrophotometer (Tecan, Baldwin Park, CA). The experiment was performed on cultures obtained from two independent dissections. The data for each biological replicate was obtained from four technical replicates, and are expressed as the mean ± SEM. Statistically significant differences between treatment groups were identified using one-way ANOVA with *post hoc* Tukey's test at $p \leq 0.05$.

2.9. Statistical analysis

The dendritic growth, cell viability and western blot analyses were performed on neurons obtained from at least two independent dissections. The number of primary dendrites and the total length of the dendritic arbor per neuron are expressed as mean ± standard error (SEM), where the mean and standard error were calculated for each condition from all independent experiments. For each biological replicate, each condition was replicated in three wells. Approximately 30–50 neurons were counted per well/condition, resulting in around 90–150 cells/condition for each experiment. Statistical significance was determined using one-way ANOVA, followed by *post hoc* Tukey's test at $P \leq 0.05$.

For axonal growth measurements, statistical analyses were performed using GraphPad Prism 9 software (San Diego, CA, USA, RRID: SCR_002798) with n being a technical replicate and alpha set to 0.05. Treatments were compared to control (BMP7) by an ANOVA with correction for multiple comparisons, either parametric (if data passed Shapiro-Wilk normality test) or nonparametric. Controls (BMP7) were compared to vehicle (C2) by a non-parametric unpaired *t*-test.

3. Results

3.1. Primary sympathetic neurons express components of the γ-secretase complex

While previous studies have examined the expression of the γ-secretase complex components in the central nervous system (Busciglio et al., 1997; Cook et al., 1996), the cellular localization of these proteins in peripheral neurons is not known. Therefore, in this study, we examined the subcellular localization of the five main components of the γ-secretase complex, presenilin (PSEN1 and PSEN 2), nicastrin, PEN2 and APH1a, using immunocytochemistry in control and BMP-7-treated cultured sympathetic neurons dissociated from embryonic rat SCG. Previous studies have shown that when grown in the absence of serum, ganglionic glial cells or BMPs, rat sympathetic neurons extend only a single axonal process; however, exposure of sympathetic neurons to BMP-7 for 5 d triggers the extension of multiple dendrites (Lein et al., 1995). We found that in sympathetic cultures grown in the absence of BMP-7, all five components of the γ-secretase complex were expressed in the cell body of sympathetic neurons (Fig. 1). In control cultures, expression for all five components was observed in the cell body and axons (Fig. 1A–E). In neurons, treated with 50 ng/ml BMP-7, co-labeling with antibody against microtubule associated protein (MAP2) confirmed that PSEN1, PSEN2, NCT and APH1a were present in dendrites of these neurons (Fig. 1A–D). PEN2 is also seen in the dendrites of BMP-7 treated neurons (arrows) (Fig. 1E). Although nuclear staining was observed with one of the PSEN1 antibodies — EP2000Y (data not shown), this staining was not observed with other PSEN1 antibodies. Unlike other members of the γ-secretase complex, NCT showed a punctate expression in the cell body and axons (Fig. 1C).

The presence of PSEN1, PSEN2 and NCT in control cultures was also confirmed using immunoblotting. Lysates from both control and BMP-7 treated cultures showed bands of similar intensity detected for PSEN1 and PSEN2 (Fig. 1F, G). A rabbit polyclonal PSEN1 antibody (D39D1) that recognizes the C-terminal region of PSEN1 showed multiple bands for PSEN1, with one around 50 kDa, which corresponds to the full-length protein, and a strong band around 20 kDa, corresponding to the C-terminal fragment (CTF) of PSEN1, suggesting that PSEN1 cleavage was observed in sympathetic neurons (Fig. 1F). The presence of the PSEN-1 CTF was confirmed by another monoclonal antibody against the C-terminal loop region (Mab 5253 — data not shown). Similarly, the PSEN2 antibody generated against the C-terminal region detected a strong band around 20 kDa, similar in molecular weight to the C-terminal fragment of PSEN2, and a weak band around 40–50 kDa, corresponding to the molecular weight of full length PSEN2 protein (Fig. 1G). Multiple bands were detected using the NCT antibody (Fig. 1H). The 90 kDa band disappeared following pre-incubation of the NCT antibody with NCT protein (data not shown), confirming the presence of NCT in control and BMP-7 treated cultures. However, we were unable to detect bands for APH1a and PEN2 in our lysates (data not shown). Despite expression of PSEN1, PSEN2 and NCT in dendrites, there was no significant quantitative difference in the expression levels of the three main components of γ-secretase in control *versus* BMP-7 treated neurons following normalization with GAPDH expression in the same samples (Fig. 1H).

3.2. Inhibition of the γ-secretase complex using PSEN 1 siRNA inhibited BMP-7-induced dendritic growth in sympathetic neurons

To test the hypothesis that the γ-secretase complex influences BMP-7-induced dendritic growth, we determined whether inhibition of this complex altered BMP-7-induced dendritic growth in sympathetic neurons isolated from E21 rat SCG neurons. In agreement with previous studies (Bruckenstein and Higgins, 1988), sympathetic neurons did not extend dendrites when cultured in defined medium in the absence of serum. However, when exposed to BMP-7 at a maximally effective concentration (50 ng/mL) for 5 d, these neurons extended multiple dendrites (Fig. 2). Transfection of SCG neurons with PSEN1 siRNA decreased cytoplasmic levels of PSEN1 protein in a subset of neurons but did not eliminate PSEN1 expression (Fig. 2A–F). However, the expression of PSEN1 siRNA significantly decreased BMP-7-induced dendritic growth (Fig. 2G–J) relative to neurons transfected with control siRNA. This was evident as a decrease in the number of primary dendrites extended per neuron, from approximately 3 dendrites per neuron in BMP-7-treated neurons transfected with control scrambled siRNA to approximately 2 dendrites per neuron in those transfected with PSEN1

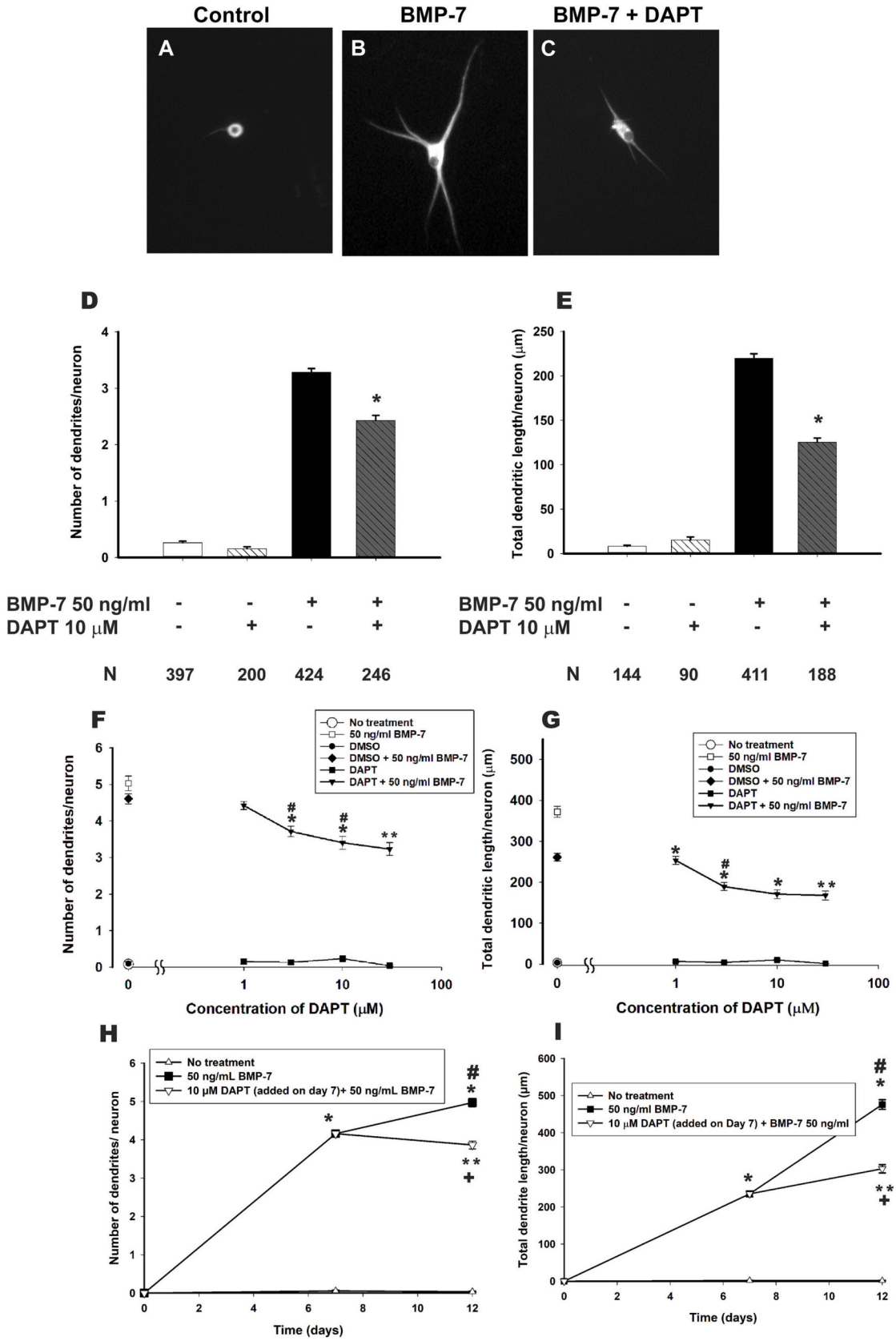

(caption on next page)

Fig. 3. Pharmacologic inhibition of γ-secretase using DAPT inhibited *de novo* BMP-7-induced dendritic growth in sympathetic neurons in a concentration dependent manner and slowed further extension of pre-existing dendrites. Sympathetic neurons were treated with DAPT (10 μM) in the presence or absence of BMP-7 (50 ng/mL) for 5 days and immunostained with an antibody against MAP-2 to visualize dendrites. Representative images of neurons treated with BMP-7 (50 ng/mL) in the presence or absence of DAPT are shown in B and C with A showing a neuron grown in the absence of BMP-7 (50 ng/mL). Dendritic growth was quantified with respect to the number of primary dendrites per neuron (D) and the total dendritic length per neuron (E). Concentration dependence was determined by treating E21 sympathetic neurons with 50 ng/ml BMP-7 in the presence or absence of DAPT (1–30 μM) for 5 days. The number of dendrites per cell (F) and the total dendritic arbor (G) were quantified in cultures immunostained for MAP-2 to identify dendritic processes. Cultures treated with BMP-7 or control media were vehicle control for 1 μM DAPT, 3 μM DAPT, 10 μM DAPT treated cultures. Neurons treated with 1:1000 DMSO (with or without BMP-7) was the vehicle control for cultures treated with 30 μM DAPT. Data are presented as the mean ± SEM. The number of cells analyzed (N) are listed in the figure for D and E, $N = 60–150$ cells per condition for F and G. Statistical significance was determined using one-way ANOVA, followed by *post hoc* Tukey's test. *Significantly different at $p \leq 0.05$ *versus* BMP-7 treated neurons. ** indicates significantly different from cultures treated with DMSO (1:1000) + BMP-7 at $p \leq 0.05$. # indicates significantly different from the next lower concentration at $p \leq 0.05$. (H, I) The effects on existing dendrites were measured by treating cultured sympathetic neurons with BMP-7 (50 ng/ml) for 7 days to induce dendritic growth, then treating for an additional 5 days with BMP-7 alone or BMP-7 plus DAPT (10 μM). Cultures were immunostained for MAP-2 and the number of dendrites/cell was quantified. Data are presented as the mean ± SD ($N = 90–180$ cells per condition). Statistical significance was assessed using one-way ANOVA, followed by Tukey's *post hoc* test. *Significantly different from cultures grown in the absence of BMP-7 at $p \leq 0.05$. #Significantly different from cultures treated with BMP-7 only for 7 days at $p \leq 0.05$. **Significantly different from cultures receiving BMP-7 alone for 7 days at $p \leq 0.05$. +Significantly different from cultures receiving BMP-7 for 12 days at $p \leq 0.05$.

siRNA (Fig. 2K). There was a significant decrease in the total length of the dendritic arbor per neuron between neurons treated with BMP-7 that were treated with only Lipofectamine® RNAiMAX (no siRNA) and BMP-7 treated neurons transfected with control scrambled siRNA, suggesting that transfection with siRNA had a negative effect on total dendritic length. However, there was no statistically significant decrease in the total dendritic arbor between BMP-7-treated neurons transfected with control scrambled siRNA and those transfected with PSEN1 (Fig. 2L).

3.3. Pharmacological inhibition of the γ-secretase complex with DAPT (GSI IX) inhibited BMP-7 induced dendritic growth

Since PSEN1 siRNA did not completely eliminate PSEN1 function and there was toxicity associated with transfection itself, we next pharmacologically inhibited γ-secretase activity using a known and well characterized γ-secretase inhibitor, DAPT (GSI IX) (Dovey et al., 2009; Oikawa et al., 2012). There was a significant decrease in the number of primary dendrites and the total dendritic arbor length in BMP-7-treated neurons exposed to DAPT (10 μM) compared to dendritic growth in BMP-7-treated neurons maintained in the absence of this inhibitor (Fig. 3A–E). Furthermore, the effects of the DAPT on the number of primary dendrites per neuron was concentration-dependent with a statistically significant decrease in the number of primary dendrites observed with 1 μM DAPT and maximal inhibition observed at 10 μM. Also, a significant decrease in the total length of the dendritic arbor was observed in cultures exposed to 1 μM DAPT. DAPT exhibited a concentration-dependent effect in BMP-7-exposed cultures with regards to both dendrite number and dendrite length, with a statistically significant decrease in total dendritic arbor length in those exposed to DAPT at 3 μM and 10 μM relative to lower concentrations of DAPT (Fig. 3F, G). Previous studies have shown that DMSO at 1:1000 dilution did not have a significant effect on dendritic growth (Chandrasekaran et al., 2000; Howard et al., 2005). Relative to neurons treated with BMP-7 in the absence of any DMSO, concurrent treatment of neurons with BMP-7 and DMSO at 1:1000 dilution (comparable to that in cultures exposed to 30 μM DAPT did not have a significant effect on dendritic numbers but significantly reduced the total length of the dendritic arbor per neuron (Fig. 3G). However, treatment with 30 μM DAPT had a significantly greater inhibitory effect on both dendritic number and dendritic length than did treatment with DMSO at 1:1000 dilution (Fig. 3F, G). In addition, exposing BMP-7-treated neurons after 7 days to 10 μM DAPT resulted in minimal further extension of dendrites and caused a statistically significant decrease in the number of primary dendrites compared to neurons in sister cultures exposed to BMP-7 for 7 days (Fig. 3H). Although the total dendritic arbor increased slightly following treatment with DAPT and BMP-7 for an additional 5 d, the overall dendritic arbor of these neurons was significantly lower than neurons treated with BMP-7 alone for 12 d (Fig. 3I).

3.4. DAPT-mediated inhibition of dendritic growth is replicated by other γ-secretase inhibitors

To confirm that the inhibition of dendritic growth was due to effects on γ-secretase activity, dendritic growth effects were tested in the presence of two additional pharmacological inhibitors of γ-secretase, LY-411575 (Wong et al., 2004) and BMS-299897 (Anderson et al., 2005).

Similar to DAPT, there was a significant decrease in the number of primary dendrites and the total dendritic arbor length in BMP-7-treated neurons exposed to LY-411575 (1 μM) or BMS-299897 (10 nM) compared to BMP-7-treated neurons maintained in the absence of these inhibitors (Fig. 4A, B). In addition, the effects of LY-411575 on the number of primary dendrites per neuron was concentration-dependent with a statistically significant decrease in the number of primary dendrites observed with 0.1 μM LY-411575 and maximal inhibition observed at 10 μM (Fig. 4C). Although the treatment of sympathetic neurons with increasing concentrations of BMS-299897 showed a trend toward increased inhibition of number of dendrites and the total dendritic arbor length compared to neurons treated with BMP-7 alone, this change was not always statistically significant compared to the next lower concentration of BMS-299897 (Fig. 4E, F). In contrast to inhibition mediated by DAPT, the inhibition of total dendritic arbor by LY-411575 (Fig. 4D) did not show concentration-dependence. DMSO, the vehicle used to dissolve LY-411575, did not have a significant effect on dendritic growth at a final dilution of 1:2000 (DMSO dilution in cultures exposed to 10 μM LY-411575).

3.5. γ-Secretase inhibitors have no effect on axonal growth or cellular health

To determine whether γ-secretase inhibitors selectively target dendrites, we evaluated the effects of these inhibitors on axonal growth. Axonal length and area of axonal coverage was measured in neurons treated with the γ-secretase inhibitors (10 μM DAPT, 1 μM LY-411575 and 3 μM BMS-299897) in the presence or absence of BMP-7 50 ng/ml for 5 days and immunostained for phosphorylated neurofilaments. The phosphorylated forms of neurofilaments are enriched in axons and their expression levels can be used as an indicator of axonal growth (Guo et al., 1998; Sternberger and Sternberger, 1983). There was no statistical difference in the axonal length or area covered by axons between BMP-7 treated cultures and cultures treated with DAPT, LY-411575 or BMS 299897 in the presence or absence of BMP-7 (Fig. 5A–L). This was also confirmed by immunoblotting for phosphorylated neurofilaments. There was no significant effect of 10 μM DAPT (Fig. 5M) or 10 μM LY-411575 (data not shown) on the level of phosphorylated neurofilaments in BMP-7-treated cultures.

To ensure that the decrease in dendritic growth was not due to

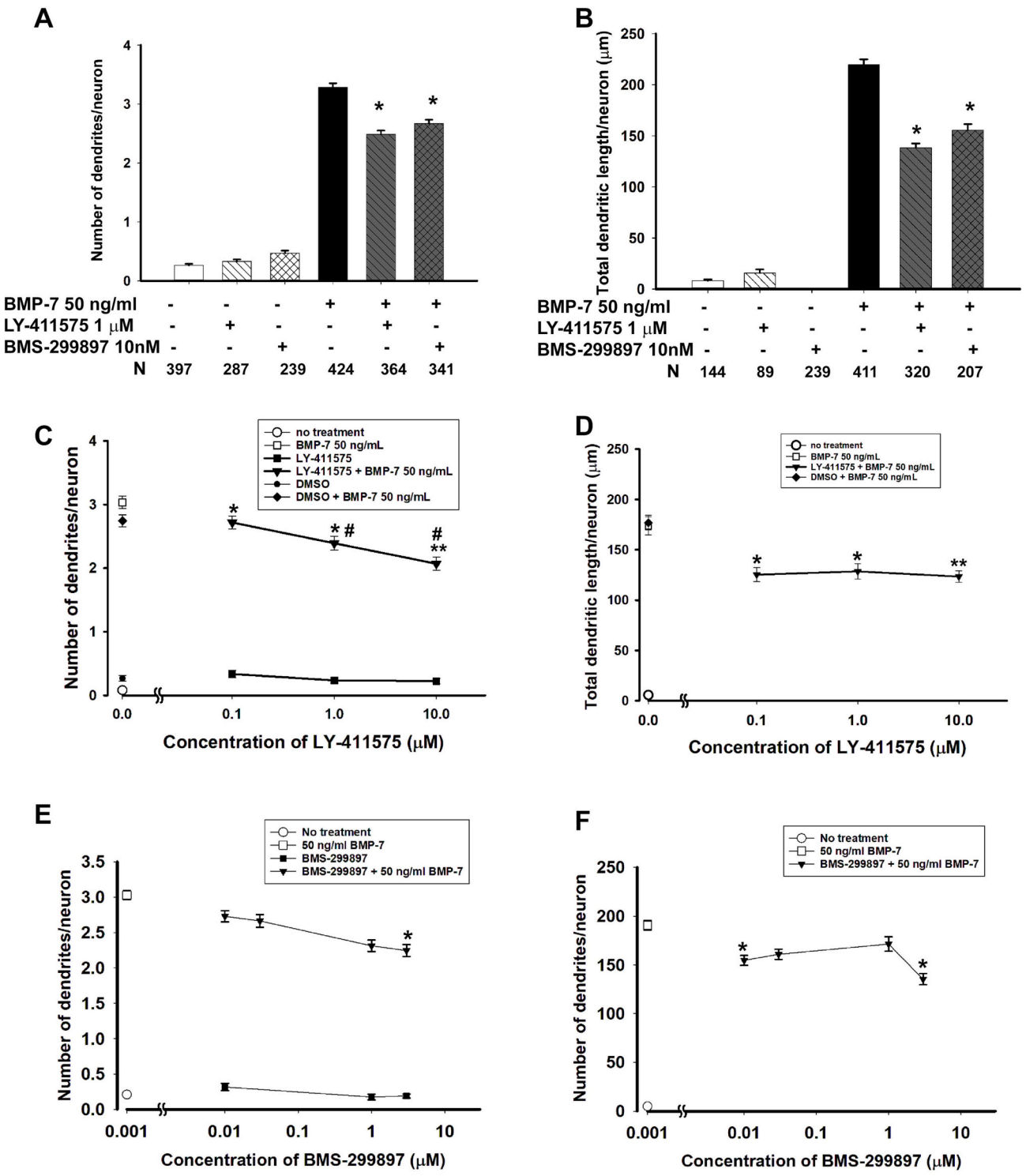

Fig. 4. Pharmacologic inhibition of γ-secretase using LY-411575 or BMS-299897 decreases BMP-7-induced dendritic growth in sympathetic neurons. Sympathetic neurons were treated with LY-411575 (1 μM) or BMS-299897 (10 nM) in the presence or absence of BMP-7 (50 ng/mL) for 5 days and immunostained with an antibody against MAP-2 to visualize dendrites. Dendritic growth was quantified with respect to the number of primary dendrites per neuron (A) and the total dendritic length per neuron (B). Data are presented as the mean ± SEM. The number of cells analyzed (N) are listed in the figure. Statistical significance was determined using one-way ANOVA, followed by *post hoc* Tukey's test. *Significantly different at $p \leq 0.05$ *versus* BMP-7 treated neurons. The concentration dependence of this inhibition was assessed by treating E21 rat SCG with 50 ng/ml BMP-7 in the presence or absence of LY-411575 (0.1–10 μM) (C, D) or BMS-299897 (10 nM–3 μM) (E, F) for 5 days. The number of dendrites per cell and the total dendritic arbor were quantified in cultures immunostained for MAP-2 to identify dendritic processes. Cultures treated with BMP-7 alone or control media were vehicle control for neurons treated with 0.1 μM LY-411575, 1 μM LY-411575 and all concentrations of BMS-299897 treated cultures. Cultures were treated with DMSO at 1:2000 was the vehicle control for 10 μM LY-411575 treated cells. Statistical significance was assessed using one-way ANOVA, followed by Tukey's *post hoc* test. (N = 200–500 per condition) * indicates significantly different from cultures treated with BMP-7 only at $p \leq 0.05$. ** indicates significantly different from cultures treated with DMSO (1:1000) + BMP-7 at $p \leq 0.05$. # indicates significantly different from the next lower concentration at $p \leq 0.05$.

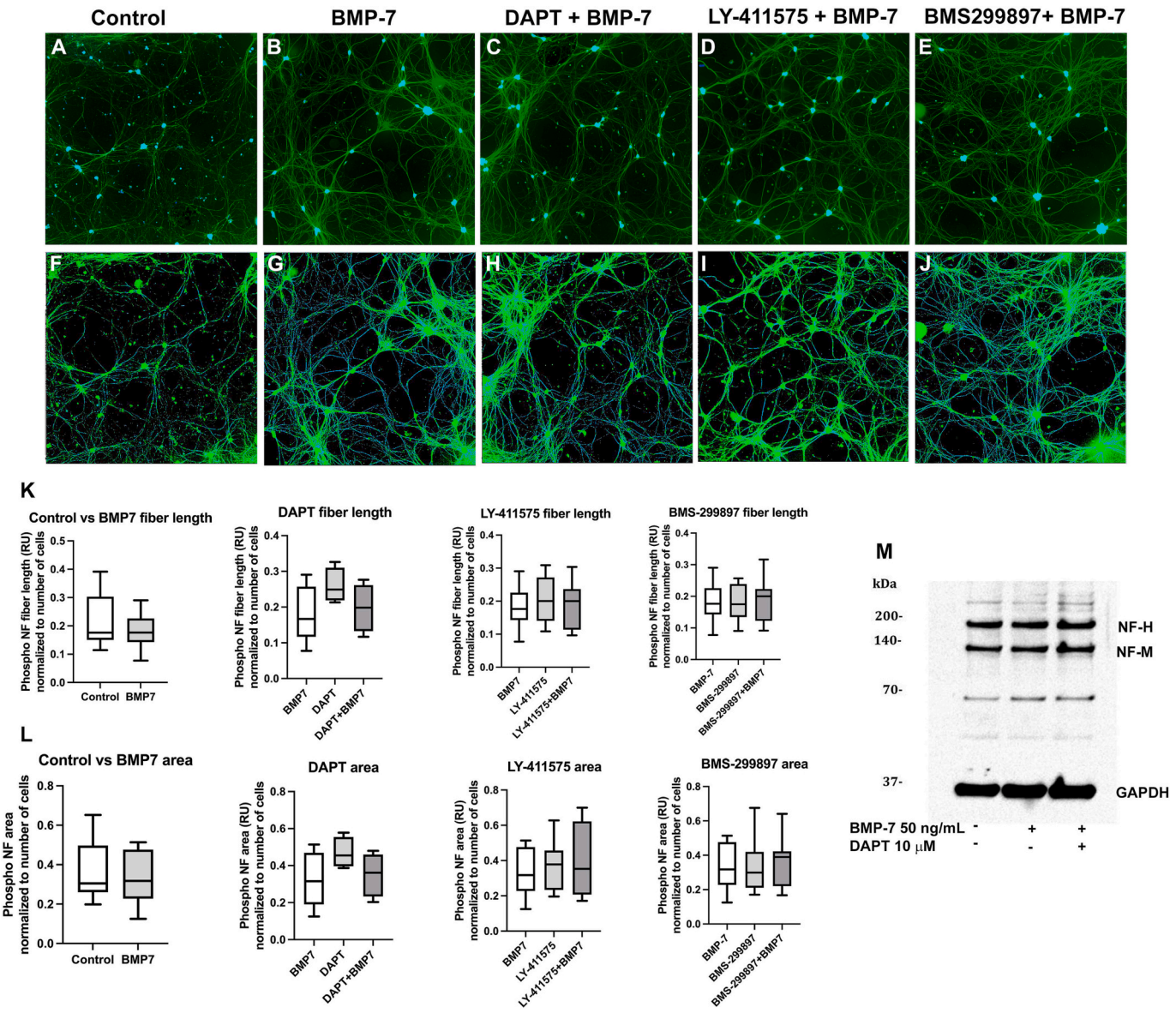

Fig. 5. γ-Secretase inhibitors do not significantly alter axonal growth.
Sympathetic neurons cultured in the absence or presence of BMP-7 (50 ng/mL) were exposed to vehicle, one of the γ-secretase inhibitors – DAPT (10 μM), LY-411575 (1 μM), or BMS-299897 (3 μM) – for 5 days, immunostained using an antibody against phosphorylated neurofilaments (phospho NF, SMI-31) and visualized by immunofluorescence. (A–E) show the staining for phospho NF in green, with blue mask for the cells. (F–J) show the same cells as in A–E with a skeletonized mask showing the axons that was used to measure axonal length and area. The quantitative comparison of axonal length and axonal area between the different conditions is shown in (K) and (L) respectively. These data were collected from randomly taken 4–19 images at 10× from each of the 3–4 coverslips per treatment. For immunoblotting, cultured sympathetic neurons were exposed to control media, BMP-7 (50 ng/ml), DAPT (10 μM) + BMP-7 (50 ng/ml) for 5 days, lysed and immunoblotted using an antibody against phosphorylated neurofilament H (SMI-31). Immunoblots were probed for GAPDH as a loading control. (M) Representative western blots probed for phosphorylated forms of NF-H (200 kDa), NF-M (160 kDa) and GAPDH (37 kDa). The experiment was repeated with lysates obtained from at least two independent dissections.

cellular toxicity, general cell health was assessed using the MTT assay, which is a measure of metabolic rate (Kim et al., 2009; van Meerloo et al., 2011). Our data confirmed previous observations that the absorbance of MTT was higher in BMP-7 treated cells compared to control cells (Chandrasekaran et al., 2015). However, the absorbance values were comparable between BMP-7-treated cultures in the absence or presence of maximum concentrations of DAPT, LY-411575 and BMS-299897 (Fig. 6).

3.6. BMP-induced SMAD nuclear translocation is not altered by γ-secretase inhibitors

Transcriptional regulation by the BMP signaling pathway is mediated by transcription factors known as SMADs. The binding of BMPs to BMP receptors results in the phosphorylation of SMAD1 and SMAD5. These SMADs then complex with SMAD4, and the SMAD1/5 and SMAD4 complex translocates to the nucleus to regulate gene expression (Massagué and Chen, 2000). To determine whether the interactions between the γ-secretase and BMP signaling pathways occur during the early stages of BMP-7 signaling, the effect of γ-secretase inhibitors on nuclear translocation of phosphorylated SMADs was examined. In neuronal cell

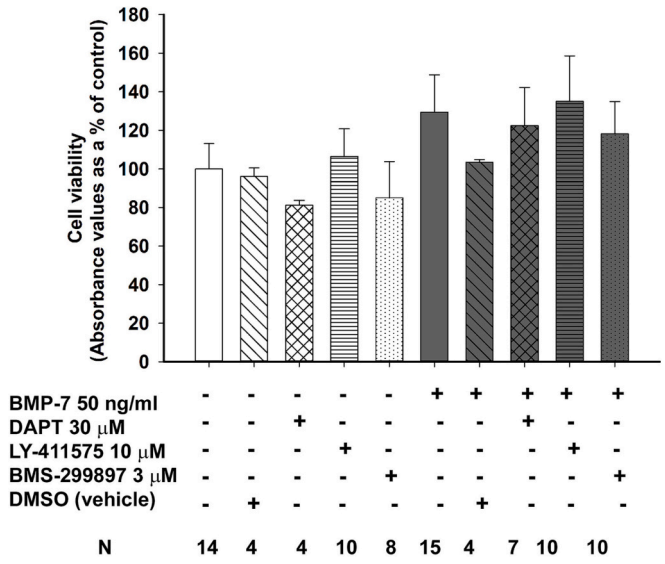

Fig. 6. γ-Secretase inhibitors do not significantly affect cellular health.
The effect of γ-secretase inhibitors on cell viability was measured using the MTT assay. Sympathetic neurons were treated with BMP-7 (50 ng/ml) in the absence or presence of either DMSO (vehicle control), DAPT (30 μM), LY-411575 (10 μM) or BMS-299897 (3 μM). Absorbance values at 570 nm are expressed as % absorbance in control cultures. Data are from three independent experiments expressed as the mean ± SEM. The number of cultures analyzed (N) are listed in the figure. As determined by one-way ANOVA ($p \leq 0.05$), there were no statistically significant differences between neurons treated under the various conditions.

cultures grown in the absence of BMP-7, phosphorylated SMADs were localized in the cytoplasm in 100 % of the neurons. In contrast, in cultures treated with BMP-7 (50 ng/mL) for 5 d, phospho-SMAD 1,5 immunoreactivity is predominantly localized to the nucleus in all neurons, and this nuclear localization was not altered by treatment with DAPT (10 μM) (Fig. 7). Similar results were obtained with LY-411575 (data not shown).

4. Discussion

Previous studies have examined the expression of the γ-secretase complex components in the central nervous system (Busciglio et al., 1997; Cook et al., 1996) and have shown that γ-secretase function is necessary for triggering apoptosis in postnatal rat sympathetic neurons (Kenchappa et al., 2006). Our data extend these observations by providing the first characterization of the subcellular localization of the four core members of the γ-secretase complex in primary sympathetic neurons. Documentation of the expression of the integral members of the complex, PSEN1/PSEN2, nicastrin, PEN2 and APH1a, in the cytoplasm of sympathetic neurons provides strong evidence for the assembly and activity of the complex in these cells. Interestingly, nicastrin exhibited a punctate staining in our neuronal cultures, suggesting synaptic localization of this protein. Previous studies have shown that nicastrin is necessary for both short-term and long-term synaptic plasticity in hippocampal neurons (Lee et al., 2014). Further studies are necessary to examine whether nicastrin has a similar function in peripheral neurons.

The γ-secretase complex has been shown to be involved in neurite outgrowth in central neurons, predominantly affecting axonal growth and dendritic spine development (Bittner et al., 2009; Carroll and Li, 2016; Duncan et al., 2018). Our study extends these observations to dendritic growth in peripheral neurons. However, unlike a previous study in which the inhibition of γ-secretase promoted dendritic outgrowth in cortical neurons (Deyts et al., 2016), we found that inhibition of the γ-secretase complex significantly decreased BMP-7-induced dendritic growth in sympathetic neurons. Also, unlike observations of central neurons, where inhibition of γ-secretase promoted axonal growth, treatment with γ-secretase inhibitors did not change the expression of phosphorylated neurofilaments, a marker for axonal growth, in sympathetic neurons, suggesting that the effects are predominantly on dendritic morphogenesis. These observations suggest a different role for this enzyme complex in peripheral neurons compared to central neurons. Interestingly, nicastrin and APH1a show strong expression in axons, while other components of the γ-secretase complex are expressed at low levels or are not detected in sympathetic axons. This observation suggests that some of the components play additional roles

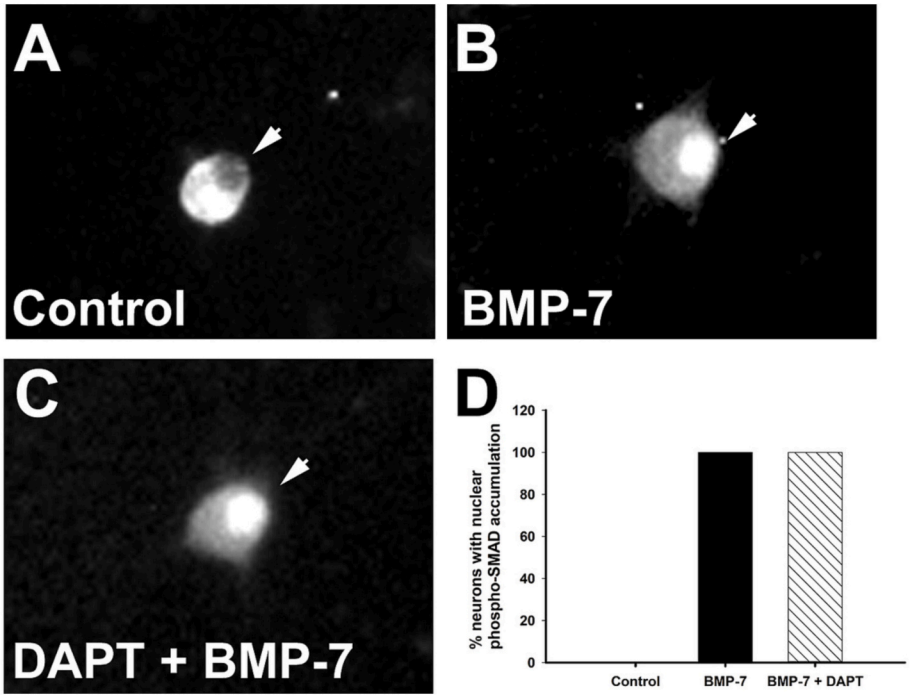

Fig. 7. DAPT did not affect BMP-induced nuclear translocation of phosphorylated SMADs. Sympathetic neurons were treated with BMP-7 (50 ng/mL) in the absence or presence of DAPT (10 μM) for 5 days and then immunostained for phosphorylated SMAD 1 and SMAD 5. Negative control cultures were maintained in the absence of BMP-7. (A–C) Representative images of P-SMAD 1,5 immunoreactivity in cells from each treatment group. (D) The percentage of neurons with nuclear staining for P-SMAD 1,5 was determined from 100 neurons in each condition. Statistical significance was assessed using one-way ANOVA, followed by *post hoc* Tukey's test. *Significantly different from negative control cultures not exposed to BMP-7 at $p \leq 0.05$.

in axonal growth and development in sympathetic neurons. Further studies are necessary to determine whether the γ-secretase complex or specific components of the complex regulate aspects of axonal growth in sympathetic neurons. Our study also showed that although DAPT did not cause significant retraction of existing dendrites, it prevents further addition of dendrites, evidenced as only a minimal increase in dendritic extension in the presence of BMP-7, suggesting that the use of γ-secretase inhibitors may prevent dendritic remodeling in peripheral neurons.

Although the inhibition of the γ-secretase pathway significantly decreased BMP-7-induced dendritic growth, neither genetic nor pharmacologic methods of inhibition completely blocked BMP-induced dendritic growth. One possible explanation of this observation is that there are multiple signaling pathways that interact with BMP-7 signaling to determine the final shape of the dendritic arbor. In support of this hypothesis, studies have shown interactions between BMP signaling and signaling by reactive oxygen species (ROS), cytokines, and growth factors modulate dendritogenesis (Chandrasekaran et al., 2015; Guo et al., 1997; Kim et al., 2002, 2009). Moreover, BMP-7 signaling has been shown to activate numerous genes during the induction of dendritic growth in sympathetic neurons (Garred et al., 2011). Since many of these genes are most likely not inhibited by γ-secretase inhibitors, the activity of these genes could be contributing to the dendritic growth observed in the cultures treated with γ-secretase inhibitors. In agreement with this, our results showed that BMP-induced nuclear translocation of SMADs was unaffected by pharmacologic inhibition of the γ-secretase signaling pathway, suggesting that early steps in the BMP-7 signaling pathway were unaffected by the presence of γ-secretase inhibitors.

Previous studies have shown that the γ-secretase complex cleaves over 90 proteins within the transmembrane domain, including APP, Notch and $p75^{NTR}$ (Haapasalo and Kovacs, 2011). Although there are numerous studies documenting the role of APP in neuronal development, intracellular transport, and synaptogenesis in central neurons, the function of APP and its cleavage products in peripheral neurons is not well understood (Puig and Combs, 2013; van der Kant and Goldstein, 2015; Zhang et al., 2021). A recent study showed that APP was highly expressed in sympathetic neurons cultured from postnatal mouse SCG and was necessary for the modulation of alpha-adrenergic receptor activity in these neurons (Zhang et al., 2017). Also, overexpression of BMP-4 in the hippocampus and different neuronal cell lines was found to increase expression of APP (Zhang et al., 2021), suggesting an interplay between BMP signaling and γ-secretase signaling in APP signaling in the nervous system. Interestingly, one of the γ-secretase inhibitors used in this study – BMS-299897 – has been shown to be 15-fold more selective for inhibition of APP cleavage than Notch (Barten et al., 2004). Our findings show that the dendrite number and total length of the dendritic arbor induced by BMP-7 were significantly decreased at concentrations of BMS-299897 that had been shown to inhibit APP processing, suggesting that activation of APP may be important for dendritic growth regulation in sympathetic neurons. Additional studies are necessary to examine whether cleavage of APP is inhibited by the inhibitors in sympathetic neurons and whether APP signaling is important for dendritic growth regulation in these neurons.

Two other targets of γ-secretase, Notch and $p75^{NTR}$, have been shown to interact with the BMP-7 signaling pathway. Notch and BMP signaling pathways are known to interact in the development of limbs, nervous system and other organ systems during embryonic development (Siebel and Lendahl, 2017; Ye and Fortini, 1999). In embryonic sympathetic neurons, Jagged, a ligand for Notch signaling, is upregulated by BMP-7 during dendritic growth initiation (Garred et al., 2011), suggesting the possibility of an interaction between BMP-7 and Notch signaling during BMP-induced dendritic growth. This also suggests that BMP and γ-secretase pathway may be working synergistically to activate the Notch pathway in sympathetic neurons with γ-secretase pathway activating Notch receptor and BMP signaling increasing the expression of the Jagged. Similarly, activation of $p75^{NTR}$ following γ-secretase cleavage has been observed in PC12 cells and postnatal superior cervical ganglia neurons. Expression of $p75^{NTR}$ is upregulated by BMP-7 and is necessary for BMP-7-induced dendritic growth in sympathetic neurons (Courter et al., 2016; Kenchappa et al., 2006; Sykes et al., 2012). Additional studies are necessary to determine whether the transcriptional regulation mediated by the intracellular domain of $p75^{NTR}$ released following γ-secretase cleavage is necessary for its dendritic growth promoting effects. Future studies will provide better characterization of the γ-secretase targets and their interaction with BMP-7 signaling during the initial stages of dendritic growth in peripheral neurons. Additional studies will also examine the synergistic relationship between BMP signaling and γ-secretase signaling in regulating these targets in sympathetic neurons.

Impairment of the autonomic nervous system has been observed in patients with Alzheimer's disease with symptoms of autonomic dysfunction including dizziness, syncope, changes in blood pressure and heart rate being closely correlated with cognitive changes during disease progression (Engelhardt and Laks, 2008; Femminella et al., 2014; Jensen-Dahm et al., 2015). Recent studies have also shown that the β-amyloid protein can induce neurotoxicity and reduce neurite outgrowth which can be ameliorated by expression of $p75^{NTR}$ in sympathetic neurons of Alzheimer's disease mice models (Bengoechea et al., 2009; Shu et al., 2015). Our data on the role of γ-secretase in sympathetic neurons provides additional evidence for the importance of this pathway in the peripheral nervous system. In addition, our data showed positive interactions between the BMP signaling and γ-secretase pathway in sympathetic neurons. Previous studies have shown an increase in the expression of BMP-6 in the brains of Alzheimer's disease patients and of APP transgenic mice (Crews et al., 2010). Further studies will help unravel the interplay between these two signaling pathways and their importance in autonomic changes observed during Alzheimer's disease progression.

5. Conclusions

In summary, our data demonstrate that members of the γ-secretase complex are expressed in sympathetic neurons cultured from embryonic rat SCG, and that inhibition of this complex significantly decreased BMP-7-induced dendritic growth in the absence of effects on axonal growth or general cell health. Furthermore, our data suggest the involvement of APP and potentially other γ-secretase targets in regulating dendritic growth in these neurons. Collectively, these data provide evidence that γ-secretase signaling enhances BMP-7-induced dendritic growth in sympathetic neurons.

Funding

This work was supported by the Saint Mary's College Summer Research Program (KK, RG), Saint Mary's College Faculty Development Fund, Faculty Research Grant and Alumni Faculty Fellowship grant (VC), the National Institute of Environmental Health Science R21 grant (grant number ES026515 to PJL), the National Institute of Aging (grant AG074709 to PJL), and Intellectual and Developmental Disabilities Research Center (IDDRC) at UC Davis (grant P50 HD103526). The funding agencies were not involved in the study design, in the collection, analysis, or interpretation of data, in the writing of the report or in the decision to submit the paper for publication.

Declaration of competing interest

The authors have no conflicts of interest to disclose.

Data availability

Data will be made available on request.

References

Anderson, J.J., Holtz, G., Baskin, P.P., Turner, M., Rowe, B., Wang, B., Kounnas, M.Z., Lamb, B.T., Barten, D., Felsenstein, K., McDonald, I., Srinivasan, K., Munoz, B., Wagner, S.L., 2005. Reductions in beta-amyloid concentrations in vivo by the gamma-secretase inhibitors BMS-289948 and BMS-299897. Biochem. Pharmacol. 69, 689–698. https://doi.org/10.1016/J.BCP.2004.11.015.

Angley, C., Kumar, M., Dinsio, K.J., Hall, A.K., Siegel, R.E., 2003. Signaling by bone morphogenetic proteins and Smad1 modulates the postnatal differentiation of cerebellar cells. J. Neurosci. 23, 260–268.

Barten, D.M., Guss, V.L., Corsa, J.A., Loo, A., Hansel, S.B., Zheng, M., Munoz, B., Srinivasan, K., Wang, B., Robertson, B.J., Polson, C.T., Wang, J., Roberts, S.B., Hendrick, J.P., Anderson, J.J., Loy, J.K., Denton, R., Verdoorn, T.A., Smith, D.W., Felsenstein, K.M., 2004. Dynamics of -amyloid reductions in brain, cerebrospinal fluid, and plasma of -amyloid precursor protein transgenic mice treated with a -secretase inhibitor. J. Pharmacol. Exp. Ther. 312, 635–643. https://doi.org/10.1124/jpet.104.075408.

Bengoechea, T.G., Chen, Z., O'Leary, D.A., Masliah, E., Lee, K.-F., Heinemann, S.F., 2009. p75 reduces ␤-amyloid-induced sympathetic innervation deficits in an Alzheimer's disease mouse model. PNAS 106, 7870–7875.

Bittner, T., Fuhrmann, M., Burgold, S., Jung, C.K.E., Volbracht, C., Steiner, H., Mitteregger, G., Kretzschmar, H.A., Haass, C., Herms, J., 2009. Gamma-secretase inhibition reduces spine density in vivo via an amyloid precursor protein-dependent pathway. J. Neurosci. 29, 10405–10409. https://doi.org/10.1523/JNEUROSCI.2288-09.2009.

Bruckenstein, D.A., Higgins, D., 1988. Morphological differentiation of embryonic rat sympathetic neurons in tissue culture. Dev. Biol. 128, 337–348. https://doi.org/10.1016/0012-1606(88)90296-5.

Busciglio, J., Hartmann, H., Lorenzo, A., Wong, C., Baumann, K., Sommer, B., Staufenbiel, M., Yankner, B.A., 1997. Neuronal localization of Presenilin-1 and association with amyloid plaques and neurofibrillary tangles in Alzheimer's disease. J. Neurosci. 17, 5101–5107.

Carroll, C.M., Li, Y.-M., 2016. Physiological and pathological roles of the γ-secretase complex. Brain Res. Bull. 126, 199–206. https://doi.org/10.1016/j.brainresbull.2016.04.019.

Chandrasekaran, V., Lea, C., Sosa, J.C., Higgins, D., Lein, P.J., 2015. Reactive oxygen species are involved in BMP-induced dendritic growth in cultured rat sympathetic neurons. Mol. Cell. Neurosci. 67, 116–125. https://doi.org/10.1016/j.mcn.2015.06.007.

Chandrasekaran, V., Lein, P.J., 2018. Regulation of dendritogenesis in sympathetic neurons. In: Autonomic Nervous System. InTech. https://doi.org/10.5772/intechopen.80480.

Chandrasekaran, V., Zhai, Y., Wagner, M., Kaplan, P.L., Napoli, J.L., Higgins, D., 2000. Retinoic acid regulates the morphological development of sympathetic neurons. J. Neurobiol. 42 https://doi.org/10.1002/(SICI)1097-4695(200003)42:4<383::AID-NEU1>3.0.CO;2-9.

Cook, D.G., Sung, J.C., Golde, T.E., Felsenstein, K.M., Wojczyk, B.S., Tanzi, R.E., Trojanowski, J.Q., Lee, V.M.-Y., Doms, R.W., 1996. Expression and analysis of presenilin 1 in a human neuronal system: localization in cell bodies and dendrites. Proc. Natl. Acad. Sci. U. S. A. 93, 9223–9228. https://doi.org/10.2307/40030.

Courter, L.A., Shaffo, F.C., Ghogha, A., Parrish, D.J., Lorentz, C.U., Habecker, B.A., Lein, P.J., 2016. BMP7-induced dendritic growth in sympathetic neurons requires p75 NTR signaling. Dev. Neurobiol. 76, 1003–1013. https://doi.org/10.1002/dneu.22371.

Crews, L., Adame, A., Patrick, C., Delaney, A., Pham, E., Rockenstein, E., Hansen, L., Masliah, E., 2010. Increased BMP6 levels in the brains of Alzheimer's disease patients and APP transgenic mice are accompanied by impaired neurogenesis. J. Neurosci. 30, 12252–12262. https://doi.org/10.1523/JNEUROSCI.1305-10.2010.

Deyts, C., Clutter, M., Herrera, S., Jovanovic, N., Goddi, A., Parent, A.T., 2016. Loss of presenilin function is associated with a selective gain of APP function. elife 5. https://doi.org/10.7554/eLife.15645.

Dovey, H.F., John, V., Anderson, J.P., Chen, L.Z., de Saint Andrieu, P., Fang, L.Y., Freedman, S.B., Folmer, B., Goldbach, E., Holsztynska, E.J., Hu, K.L., Johnson-Wood, K.L., Kennedy, S.L., Kholodenko, D., Knops, J.E., Latimer, L.H., Lee, M., Liao, Z., Lieberburg, I.M., Motter, R.N., Mutter, L.C., Nietz, J., Quinn, K.P., Sacchi, K. L., Seubert, P.A., Shopp, G.M., Thorsett, E.D., Tung, J.S., Wu, J., Yang, S., Yin, C.T., Schenk, D.B., May, P.C., Altstiel, L.D., Bender, M.H., Boggs, L.N., Britton, T.C., Clemens, J.C., Czilli, D.L., Dieckman-McGinty, D.K., Droste, J.J., Fuson, K.S., Gitter, B.D., Hyslop, P.A., Johnstone, E.M., Li, W.-Y., Little, S.P., Mabry, T.E., Miller, F.D., Ni, B., Nissen, J.S., Porter, W.J., Potts, B.D., Reel, J.K., Stephenson, D., Su, Y., Shipley, L.A., Whitesitt, C.A., Yin, T., Audia, J.E., 2009. Functional gamma-secretase inhibitors reduce beta-amyloid peptide levels in brain. J. Neurochem. 76, 173–181. https://doi.org/10.1046/j.1471-4159.2001.00012.x.

D'Souza, Y., Elharram, A., Soon-Shiong, R., Andrew, R.D., Bennett, B.M., 2015. Characterization of Aldh2 (-/-) mice as an age-related model of cognitive impairment and Alzheimer's disease. Mol. Brain 8, 27. https://doi.org/10.1186/s13041-015-0117-y.

Duncan, R.S., Song, B., Koulen, P., 2018. Presenilins as drug targets for Alzheimer's disease-recent insights from cell biology and electrophysiology as novel opportunities in drug development. Int. J. Mol. Sci. 19 https://doi.org/10.3390/ijms19061621.

Engelhardt, E., Laks, J., 2008. Alzheimer disease neuropathology: understanding autonomic dysfunction. Dement. Neuropsychol. 2, 183–191.

Esquenazi, S., Monnerie, H., Kaplan, P., le Roux, P., 2002. BMP-7 and excess glutamate: opposing effects on dendrite growth from cerebral cortical neurons in vitro. Exp. Neurol. 176, 41–54. https://doi.org/10.1006/exnr.2002.7906.

Femminella, G.D., Rengo, G., Komici, K., Iacotucci, P., Petraglia, L., Pagano, G., de Lucia, C., Canonico, V., Bonaduce, D., Leosco, D., Ferrara, N., 2014. Autonomic dysfunction in Alzheimer's disease: tools for assessment and review of the literature. J. Alzheimers Dis. 42, 369–377. https://doi.org/10.3233/JAD-140513.

Francis, R., McGrath, G., Zhang, J., Ruddy, D.A., Sym, M., Apfeld, J., Nicoll, M., Maxwell, M., Hai, B., Ellis, M.C., Parks, A.L., Xu, W., Li, J., Gurney, M., Myers, R.L., Himes, C.S., Hiebsch, R., Ruble, C., Nye, J.S., Curtis, D., 2002. Aph-1 and pen-2 are required for notch pathway signaling, gamma-secretase cleavage of betaAPP, and presenilin protein accumulation. Dev. Cell 3, 85–97. https://doi.org/10.1016/S1534-5807(02)00189-2.

Garred, M.M., Wang, M.M., Guo, X., Harrington, C.A., Lein, P.J., 2011. Transcriptional responses of cultured rat sympathetic neurons during BMP-7-induced dendritic growth. PLoS One 6, e21754.

Ghogha, A., Bruun, D.a., Lein, P.J., 2012. Inducing dendritic growth in cultured sympathetic neurons. J. Vis. Exp. 4–8. https://doi.org/10.3791/3546.

Granholm, A.C., Sanders, L.A., Ickes, B., Albeck, D., Hoffer, B.J., Young, D.A., Kaplan, P. L., 1999. Effects of osteogenic protein-1 (OP-1) treatment on fetal spinal cord transplants to the anterior chamber of the eye. Cell Transplant. 8, 75–85.

Gratacos, E., Checa, N., Perez-Navarro, E., Alberch, J., 2008. Brain-derived neurotrophic factor (BDNF) mediates bone morphogenetic protein-2 (BMP-2) effects on cultured striatal neurons. J. Neurochem. 79, 747–755. https://doi.org/10.1046/j.1471-4159.2001.00570.x.

Gu, Y., Sanjo, N., Chen, F., Hasegawa, H., Petit, A., Ruan, X., Li, W., Shier, C., Kawarai, T., Schmitt-Ulms, G., Westaway, D., St George-Hyslop, P., Fraser, P.E., 2004. The presenilin proteins are components of multiple membrane-bound complexes that have different biological activities. J. Biol. Chem. 279, 31329–31336. https://doi.org/10.1074/jbc.M401548200.

Guo, X., Metzler-Northrup, J., Lein, P., Rueger, D., Higgins, D., 1997. Leukemia inhibitory factor and ciliary neurotrophic factor regulate dendritic growth in cultures of rat sympathetic neurons. Dev. Brain Res. 104, 101–110. https://doi.org/10.1016/S0165-3806(97)00142-9.

Guo, X., Rueger, D., Higgins, D., 1998. Osteogenic protein-1 and related bone morphogenetic proteins regulate dendritic growth and the expression of microtubule-associated protein-2 in rat sympathetic neurons. Neurosci. Lett. 245, 131–134.

Haapasalo, A., Kovacs, D.M., 2011. The many substrates of presenilin/γ-secretase. J. Alzheimers Dis. 25, 3–28. https://doi.org/10.3233/JAD-2011-101065.

Haass, C., de Strooper, B., 1999. The presenilins in Alzheimer's disease-proteolysis holds the key. Science 1979, 286.

Hane, F.T., Lee, B.Y., Leonenko, Z., 2017. Recent progress in Alzheimer's disease research, part 1: pathology. J. Alzheimers Dis. 57, 1–28. https://doi.org/10.3233/JAD-160882.

Hocking, J.C., Hehr, C.L., Chang, R.-Y., Johnston, J., McFarlane, S., 2008. TGFβ ligands promote the initiation of retinal ganglion cell dendrites in vitro and in vivo. Mol. Cell. Neurosci. 37, 247–260. https://doi.org/10.1016/j.mcn.2007.09.011.

Holt, M., Adams, B., Chandrasekaran, V., 2020. Culturing rat sympathetic neurons from embryonic superior cervical ganglia for morphological and proteomic analysis. J. Vis. Exp. 2020, e61283 https://doi.org/10.3791/61283.

Howard, A.S., Bucelli, R., Jett, D.A., Bruun, D., Yang, D., Lein, P.J., 2005. Chlorpyrifos exerts opposing effects on axonal and dendritic growth in primary neuronal cultures. Toxicol. Appl. Pharmacol. 207, 112–124. https://doi.org/10.1016/J.TAAP.2004.12.008.

Issac, T.G., Chandra, S.R., Gupta, N., Rukmani, M.R., Deepika, S., Sathyaprabha, T.N., 2017. Autonomic dysfunction: a comparative study of patients with Alzheimer's and frontotemporal dementia - a pilot study. J. Neurosci. Rural Pract. 8, 84–88. https://doi.org/10.4103/0976-3147.193545.

Jensen-Dahm, C., Waldemar, G., Staehelin Jensen, T., Malmqvist, L., Moeller, M.M., Andersen, B.B., Høgh, P., Ballegaard, M., 2015. Autonomic dysfunction in patients with mild to moderate Alzheimer's disease. J. Alzheimers Dis. 47, 681–689. https://doi.org/10.3233/JAD-150169.

Kenchappa, R.S., Zampieri, N., Chao, M.v., Barker, P.A., Teng, H.K., Hempstead, B.L., Carter, B.D., 2006. Ligand-dependent cleavage of the P75 neurotrophin receptor is necessary for NRIF nuclear translocation and apoptosis in sympathetic neurons. Neuron 50, 219–232. https://doi.org/10.1016/j.neuron.2006.03.011.

Kim, I.-J., Beck, H.N., Lein, P.J., Higgins, D., 2002. Interferon gamma induces retrograde dendritic retraction and inhibits synapse formation. J. Neurosci. 22, 4530–4539 doi: 20026431.

Kim, W.-Y., Gonsiorek, E.A., Barnhart, C., Davare, M.A., Engebose, A.J., Lauridsen, H., Bruun, D., Lesiak, A., Wayman, G., Bucelli, R., Higgins, D., Lein, P.J., 2009. Statins decrease dendritic arborization in rat sympathetic neurons by blocking RhoA activation. J. Neurochem. 108, 1057–1071.

le Roux, P., Behar, S., Higgins, D., Charette, M., 1999. OP-1 enhances dendritic growth from cerebral cortical neurons in vitro. Exp. Neurol. 160, 151–163. https://doi.org/10.1006/exnr.1999.7194.

Lee, D., Aoki, C., 2012. Presenilin conditional double knockout mice exhibit decreases in drebrin A at hippocampal CA1 synapses. Synapse 66, 870–879. https://doi.org/10.1002/syn.21578.

Lee, S.H., Sharma, M., Südhof, T.C., Shen, J., 2014. Synaptic function of nicastrin in hippocampal neurons. Proc. Natl. Acad. Sci. U. S. A. 111, 8973–8978. https://doi.org/10.1073/pnas.1408554111.

Lein, P., Johnson, M., Guo, X., Rueger, D., Higgins, D., 1995. Osteogenic protein-1 induces dendritic growth in rat sympathetic neurons. Neuron 15, 597–605.

Lein, P.J., Guo, X., Shi, G.X., Moholt-Siebert, M., Bruun, D., Andres, D.A., 2007. The novel GTPase Rit differentially regulates axonal and dendritic growth. J. Neurosci. 27, 4725–4736. https://doi.org/10.1523/JNEUROSCI.5633-06.2007.

Li, D., Tang, J., Xu, H., Fan, X., Bai, Y., Yang, L., 2008. Decreased hippocampal cell proliferation correlates with increased expression of BMP4 in the APPswe/PS1ΔE9 mouse model of Alzheimer's disease. Hippocampus 18, 692–698. https://doi.org/10.1002/hipo.20428.

Li, Y., Lu, S.H.-J., Tsai, C.-J., Bohm, C., Qamar, S., Dodd, R.B., Meadows, W., Jeon, A., McLeod, A., Chen, F., Arimon, M., Berezovska, O., Hyman, B.T., Tomita, T., Iwatsubo, T., Johnson, C.M., Farrer, L.A., Schmitt-Ulms, G., Fraser, P.E., St George-Hyslop, P.H., 2014. Structural interactions between inhibitor and substrate docking sites give insight into mechanisms of human PS1 complexes. Structure 22, 125–135. https://doi.org/10.1016/j.str.2013.09.018.

Majdazari, A., Stubbusch, J., Müller, C.M., Hennchen, M., Weber, M., Deng, C.-X., Mishina, Y., Schütz, G., Deller, T., Rohrer, H., 2013. Dendrite complexity of sympathetic neurons is controlled during postnatal development by BMP signaling. J. Neurosci. 33, 15132–15144. https://doi.org/10.1523/JNEUROSCI.4748-12.2013.

Massagué, J., Chen, Y.G., 2000. Controlling TGF-beta signaling. Genes Dev. 14, 627–644. https://doi.org/10.1101/gad.14.6.627.

Oikawa, N., Goto, M., Ikeda, K., Taguchi, R., Yanagisawa, K., 2012. The γ-secretase inhibitor DAPT increases the levels of gangliosides at neuritic terminals of differentiating PC12 cells. Neurosci. Lett. 525, 49–53. https://doi.org/10.1016/J.NEULET.2012.07.027.

Puig, K.L., Combs, C.K., 2013. Expression and function of APP and its metabolites outside the central nervous system. Exp. Gerontol. 48, 608–611. https://doi.org/10.1016/j.exger.2012.07.009.

Saura, C.A., Choi, S.-Y., Beglopoulos, V., Malkani, S., Zhang, D., Shankaranarayana Rao, B.S., Chattarji, S., Kelleher, R.J., Kandel, E.R., Duff, K., Kirkwood, A., Shen, J., 2004. Loss of presenilin function causes impairments of memory and synaptic plasticity followed by age-dependent neurodegeneration. Neuron 42, 23–36. https://doi.org/10.1016/S0896-6273(04)00182-5.

Shu, Y.-H., Lu, X.-M., Wei, J.-X., Xiao, L., Wang, Y.-T., 2015. Update on the role of p75NTR in neurological disorders: a novel therapeutic target. Biomed. Pharmacother. 76, 17–23. https://doi.org/10.1016/J.BIOPHA.2015.10.010.

Siebel, C., Lendahl, U., 2017. Notch signaling in development, tissue homeostasis, and disease. Physiol. Rev. 97, 1235–1294. https://doi.org/10.1152/physrev.00005.2017.

Sternberger, L.A., Sternberger, N.H., 1983. Monoclonal antibodies distinguish phosphorylated and nonphosphorylated forms of neurofilaments in situ. Proc. Natl. Acad. Sci. U. S. A. 80, 6126–6130.

Sykes, A.M., Palstra, N., Abankwa, D., Hill, J.M., Skeldal, S., Matusica, D., Venkatraman, P., Hancock, J.F., Coulson, E.J., 2012. The effects of transmembrane sequence and dimerization on cleavage of the p75 neurotrophin receptor by γ-secretase. J. Biol. Chem. 287, 43810–43824. https://doi.org/10.1074/jbc.M112.382903.

Tanzi, R.E., Bertram, L., Hannequin, D., Enghild, J., Salvesen, G.S., Roses, A.D., Hall, J.L., Saunders, A.M., Roses, A.D., 2001. New frontiers in Alzheimer's disease genetics. al., et Neuron 32, 181–184. https://doi.org/10.1016/S0896-6273(01)00476-7.

van Meerloo, J., Kaspers, G.J.L., Cloos, J., 2011. Cell sensitivity assays: the MTT assay. Methods Mol. Biol. 731, 237–245. https://doi.org/10.1007/978-1-61779-080-5_20.

van der Kant, R., Goldstein, L.S.B., 2015. Cellular functions of the amyloid precursor protein from development to dementia. Dev. Cell 32, 502–515. https://doi.org/10.1016/j.devcel.2015.01.022.

Wang, D.B., Kinoshita, Y., Kinoshita, C., Uo, T., Sopher, B.L., Cudaback, E., Keene, C.D., Bilousova, T., Gylys, K., Case, A., Jayadev, S., Wang, H.-G., Garden, G.A., Morrison, R.S., 2015. Loss of endophilin-B1 exacerbates Alzheimer's disease pathology. Brain 138, 2005–2019. https://doi.org/10.1093/brain/awv128.

Withers, G.S., Higgins, D., Charette, M., Banker, G., 2000. Bone morphogenetic protein-7 enhances dendritic growth and receptivity to innervation in cultured hippocampal neurons. Eur. J. Neurosci. 12, 106–116. https://doi.org/10.1046/j.1460-9568.2000.00889.x.

Wolfe, M.S., 2002. APP, notch, and presenilin: molecular pieces in the puzzle of Alzheimer's disease. Int. Immunopharmacol. 2, 1919–1929. https://doi.org/10.1016/S1567-5769(02)00179-0.

Wong, G.T., Manfra, D., Poulet, F.M., Zhang, Q., Josien, H., Bara, T., Engstrom, L., Pinzon-Ortiz, M., Fine, J.S., Lee, H.-J.J., Zhang, L., Higgins, G.A., Parker, E.M., 2004. Chronic treatment with the gamma-secretase inhibitor LY-411,575 inhibits beta-amyloid peptide production and alters lymphopoiesis and intestinal cell differentiation. J. Biol. Chem. 279, 12876–12882. https://doi.org/10.1074/jbc.M311652200.

Ye, Y., Fortini, M.E., 1999. Apoptotic activities of wild-type and Alzheimer's disease-related mutant presenilins in Drosophila melanogaster. J. Cell Biol. 146.

Zhang, F., Gannon, M., Chen, Y., Zhou, L., Jiao, K., Wang, Q., 2017. The amyloid precursor protein modulates α2A-adrenergic receptor endocytosis and signaling through disrupting arrestin 3 recruitment. FASEB J. 31, 4434–4446. https://doi.org/10.1096/fj.201700346R.

Zhang, F., Zhong, R., Qi, H., Li, S., Cheng, C., Liu, X., Liu, Y., Le, W., 2018. Impacts of acute hypoxia on Alzheimer's disease-like pathologies in APPswe/PS1dE9 mice and their wild type littermates. Front. Neurosci. 12, 314. https://doi.org/10.3389/fnins.2018.00314.

Zhang, X., Li, J., Li, M., Xu, H., Cao, Y., Liang, W., Ma, J., Wang, Z.P., Li, Y., 2021. BMP4 overexpression induces the upregulation of APP/Tau and memory deficits in Alzheimer's disease. Cell Death Discov. 7, 51. https://doi.org/10.1038/s41420-021-00435-x.

Zhang, X., Li, Y., Xu, H., Zhang, Y.-W., 2014. The γ-secretase complex: from structure to function. Front. Cell. Neurosci. 8, 427. https://doi.org/10.3389/fncel.2014.00427.

Zoltowska, K.M., Berezovska, O., 2017. Dynamic nature of presenilin1/?-secretase: implication for Alzheimer?s disease pathogenesis. Mol. Neurobiol. 1–10. https://doi.org/10.1007/s12035-017-0487-5.